Growth and characterization of highly mismatched $GaN_{1-x}Sb_x$ alloys

K. M. Yu,[1] S. V. Novikov,[2] Min Ting,[1,3] W. L. Sarney,[4] S. P. Svensson,[4] M. Shaw,[5] R. W. Martin,[5] W. Walukiewicz,[1] and C. T. Foxon[2]
[1]*Materials Sciences Division, Lawrence Berkeley National Laboratory, 1 Cyclotron Road, Berkeley, California 94720, USA*
[2]*School of Physics and Astronomy, University of Nottingham, Nottingham NG7 2RD, United Kingdom*
[3]*Department of Mechanical Engineering, University of California, Berkeley, California 94720, USA*
[4]*US Army Research Laboratory, 2800 Powder Mill Road, Adelphi, Maryland 20783, USA*
[5]*Department of Physics, SUPA, University of Strathclyde, Glasgow G4 0NG, United Kingdom*

(Received 24 July 2014; accepted 12 September 2014; published online 24 September 2014)

A systematic investigation on the effects of growth temperature, Ga flux, and Sb flux on the incorporation of Sb, film structure, and optical properties of the $GaN_{1-x}Sb_x$ highly mismatched alloys (HMAs) was carried out. We found that the direct bandgap ranging from 3.4 eV to below 1.0 eV for the alloys grown at low temperature. At the growth temperature of 80 °C, $GaN_{1-x}Sb_x$ with $x > 6\%$ losses crystallinity and becomes primarily amorphous with small crystallites of 2–5 nm. Despite the range of microstructures found for $GaN_{1-x}Sb_x$ alloys with different composition, a well-developed absorption edge shifts from 3.4 eV (GaN) to close to 2 eV for samples with a small amount, less than 10% of Sb. Luminescence from dilute $GaN_{1-x}Sb_x$ alloys grown at high temperature and the bandgap energy for alloys with higher Sb content are consistent with a localized substitutional Sb level E_{Sb} at ~1.1 eV above the valence band of GaN. The decrease in the bandgap of $GaN_{1-x}Sb_x$ HMAs is consistent with the formation of a Sb-derived band due to the anticrossing interaction of the Sb states with the valence band of GaN. © *2014 AIP Publishing LLC*. [http://dx.doi.org/10.1063/1.4896364]

I. INTRODUCTION

We have recently suggested that group III-nitride highly mismatched alloys (HMAs) have electronic and optical properties suitable for photoelectrodes for the direct conversion of sunlight into hydrogen by photoelectrochemical (PEC) water-splitting.[1,2] HMAs are a new class of compound semiconductor alloys in which the anions are partially replaced by elements with very different electronegativity and/or atomic size (e.g., N in GaAs or As in GaN).[3] Due to the large mismatch of the component materials, the synthesis of HMAs is difficult and requires non-equilibrium growth conditions. However, it has been shown that substituting a very small fraction of the anions can result in a strong modification of the electronic band structure of the conduction or the valence band. The band structure modifications are well described by the Band Anticrossing (BAC) model, which considers the interaction between localized states of the minority anions and the extended states of the host compound.[3–5] The dispersion relations of the modified conduction or valence band are given by the solutions of the BAC equation,[3–5]

$$E_{\pm}(k) = \frac{1}{2}(E_d + E(k)) \pm \sqrt{(E(k) - E_d)^2 + 4C^2x}, \qquad (1)$$

where E_d is the energy of localized impurity level, $E(k)$ is the matrix conduction or valence band dispersion, C is the coupling constant, and x is the impurity composition. Substitution of a more (less) electronegative anion species, e.g., N in GaAs or GaSb (As or Sb in GaN) results in the introduction of localized levels close to the conduction (valence) band. Interactions of these localized states with the extended conduction (valence) band states strongly modified the conduction (valence) band resulting in splitting the band into two sub-bands, E_- and E_+.

The large changes in the conduction or valence band structure provide a unique means to tailor the properties of HMAs to specific device applications. Notable examples of HMAs that have been explored in recent years include dilute N As-rich[4–8] and dilute As N-rich $GaN_{1-x}As_x$ (Refs. 9, 10, and 11) as well as dilute O Te-rich ZnO_xTe_{1-x}.[12] In the case of N-rich $GaN_{1-x}As_x$ and $GaN_{1-x}Sb_x$ alloys, the BAC interaction of localized As and Sb states with the valence band of GaN results in a large upward shift of the highest valence band edge and a rapid reduction of the band gap of the resulting alloys.[11,13]

Recently, we overcame the miscibility gap of GaAs and GaN alloys and synthesized $GaN_{1-x}As_x$ alloys over the whole composition range on sapphire and glass substrates using low temperature molecular beam epitaxy (LT-MBE).[2,14,15] We found that the alloys are amorphous in the composition range of $0.17 < x < 0.75$ and crystalline outside this region. The amorphous films have a smooth morphology, homogeneous composition, and sharp, well defined optical absorption edges. The bandgap energy varies in a broad energy range from ~3.4 eV in GaN to ~0.8 eV at $x \sim 0.85$ and was found to be in good agreement with predictions from the BAC model.

Since the anion mismatch is even larger between Sb and N, BAC calculations on the electronic band structure of the $GaN_{1-x}Sb_x$ alloys predict that less than 6% of Sb is needed to achieve an alloy with a bandgap ~2.2 eV with the conduction band minimum (CBM) and the valence band maximum (VBM) still straddling the water redox potentials. Hence,

$GaN_{1-x}Sb_x$ HMAs could be suitable as photoelectrodes for photoelectrochemical water splitting applications.[16] Previously, we reported the synthesis of $GaN_{1-x}Sb_x$ HMAs using low temperature plasma assisted molecular beam epitaxy (LT-PAMBE). We demonstrated that the fundamental band gap, as well as the energies of the CBM and VBM, can be controlled with the alloy composition in $GaN_{1-x}Sb_x$.[2,17,18] At a growth temperature of 80 °C, the films with $x > 0.06$ lose crystallinity and become primarily amorphous with small crystallites of 2–5 nm in size. Despite the range of microstructures found for $GaN_{1-x}Sb_x$ alloys with different composition, a well-developed optical absorption edge shifts from 3.4 eV (GaN) to close to 2.4 eV for samples with a small amount of Sb, x. In this work, we present a systematic investigation of the growth and properties of $GaN_{1-x}Sb_x$ alloys under different growth conditions using PAMBE.

II. EXPERIMENTAL DETAILS

In order to incorporate substantial amounts of Sb into GaN, we grew N-rich dilute Sb samples on (0001) sapphire substrates by plasma-assisted MBE in a MOD-GENII system at thermocouple temperatures ranging from 80 °C to 600 °C, significantly below the normal MBE nitride substrate growth temperature of ~800 °C. In MBE, the substrate temperature is normally measured using an optical pyrometer, however, because we have used uncoated transparent sapphire wafers, the pyrometer measures the temperature of the substrate heater, not that of the substrate. Therefore, in this study, our estimates of the growth temperature are based on readings of a thermocouple in contact with the substrate. A HD-25 Oxford Applied Research RF activated plasma source is used to provide active nitrogen. In this work, a constant N flux (total N beam equivalent pressure (BEP) $\sim 1.5 \times 10^{-5}$ Torr with RF power 200 W) was maintained for all growths. Elemental Ga and Sb are used as the group III- and group V metal sources. The surface reconstruction is monitored with reflection high-energy electron diffraction (RHEED).

Prior to the growth of the $GaN_{1-x}Sb_x$ layers, the sapphire wafers were annealed in 700 °C for 20 min. After annealing, the substrate was cooled down to the growth temperature over a 20 min period under a reduced active nitrogen flux and growth was initiated by simultaneous opening of the Ga and N shutters. The Sb shutter was opened after a 1 min delay in order to avoid the deposition of any Sb on the sapphire surface before GaN growth. The growth time was kept constant at 2 h for all layers. In our previous studies on $GaN_{1-x}Bi_x$, we established that, in order to incorporate a significant amount of Bi into GaN, the MBE growth temperature needs to be very low.[19] In the present study, we also investigate the effects of substrate temperatures on the structural and optical properties of $GaN_{1-x}Sb_x$. The samples were categorized into two groups: (1) high temperature growth $T_g > 500$ °C where incorporation of Sb is limited to <1%; and (2) low temperature growth with T_g in the range of 80 to 500 °C where incorporation of Sb is larger than >1%. Moreover, to study the effects of the material stoichiometry we also vary the Ga flux (BEP from 1.5×10^{-7} to 3×10^{-7} T). Crystallinity of the grown layers was studied *in situ* using RHEED and *ex situ* using x-ray diffraction (XRD). The concentration of Sb in $GaN_{1-x}Sb_x$ layers was measured using Rutherford backscattering spectrometry (RBS) with a 3.04 MeV He^{++} beam, secondary ion mass spectrometry (SIMS) using Cameca IMS-3F and IMS-4F systems, and by electron probe microanalysis (EPMA) using a Cameca SX100 apparatus. The EPMA also provides a platform for cathodoluminescence (CL) spectroscopy and mapping. The microstructural morphology of the alloys was examined with transmission electron microscopy (TEM). Microscopic crystallinity and phase separation were studied by directly comparing the selected area electron diffraction patterns (SAD) and high resolution microscopy. The band gap of the thin films was measured by optical transmission and reflection using a Perkin Elmer Lambda 950 Spectrophotometer over the wavelength range of 190–3000 nm.

III. RESULTS AND DISCUSSION

A. Effect of substrate temperature

It is known that in MBE the As solubility limit in $GaN_{1-x}As_x$ alloys increases with decreasing growth temperature.[2,14,20] Previously, we found that growth of $GaN_{1-x}As_x$ with $x > 0.02$ under Ga-rich growth conditions and at relatively high temperatures of ~600 °C results in phase separation into N-rich and As-rich phases.[2] Since Sb and N are even more mismatched in size and electronegativity than As and N, we expect that the incorporation of Sb in the N sublattice will be even more challenging. Figure 1 shows the Sb content in $GaN_{1-x}Sb_x$ films as a function of growth temperature T_g under both N-rich (Ga BEP $\sim 1.6 \times 10^{-7}$ T, Sb $\sim 9 \times 10^{-8}$ T) and Ga-rich (Ga BEP $\sim 2.2 \times 10^{-7}$ T, Sb BEP $\sim 3 \times 10^{-8}$ T) conditions. We observe that at constant Sb BEP, the Sb content is rather insensitive to the growth

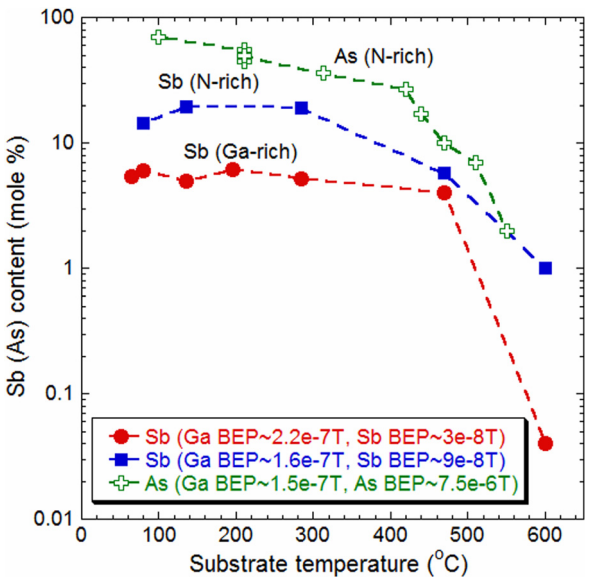

FIG. 1. Mole percent of Sb incorporated in GaN films as a function of growth temperature under both N-rich (Ga BEP $\sim 1.5 \times 10^{-7}$ T) and Ga-rich (Ga BEP $\sim 2.2 \times 10^{-7}$ T) conditions. The dependence of As content in $GaN_{1-x}As_x$ on growth temperature under N-rich condition is also shown for comparison.

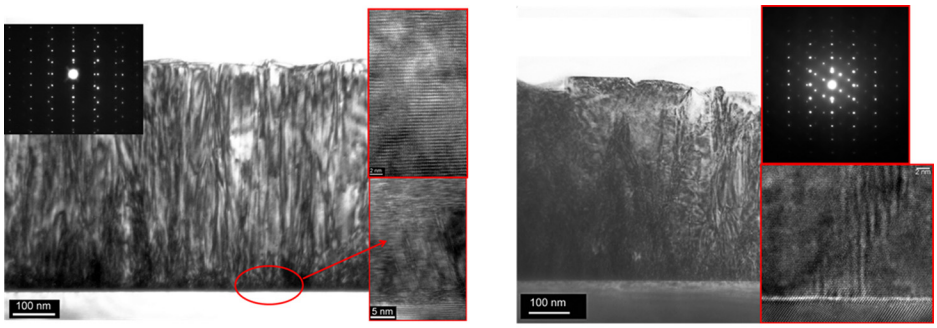

FIG. 2. TEM images of a (a) GaN film and a (b) GaNSb film with ~0.04% Sb grown at ~600 °C under Ga-rich condition (Ga BEP ~ 2.3×10^{-7} T). Selected area electron diffraction patterns are also shown in the insets of the corresponding figures.

temperature over the large temperature range 60 °C < T_g < 400 °C. This is particularly true for films grown under the Ga-rich condition. Note that the samples grown under N-rich conditions have a 3 times higher Sb BEP that results in 3–4 times higher Sb content in the films. At T_g > 500 °C, the decrease in Sb content with increasing T_g is even more pronounced when the films were grown under Ga-rich conditions. For example, at T_g ~ 600 °C, only ~ 0.04% of Sb was incorporated. These results can be contrasted with the growth of $GaN_{1-x}As_x$ HMAs that, as shown in Fig. 1, exhibits a stronger effect of temperature on the As content for T_g < 400 °C.[2]

B. High temperature growth

According to the BAC model, the electronic structure of $GaN_{1-x}Sb_x$ alloys is determined by interactions between localized states of Sb and the extended states of the GaN host matrix. The approximate location of the Sb level in GaN can be deduced from its known position at 1.0 eV below the VBM of GaAs.[13] Considering that the valence band edge offset between GaAs and GaN equals 2 eV, this places the Sb level at about 1 eV above the VBM of GaN. To better locate the position of the Sb level in GaN, we have grown a series of epitaxial GaN:Sb samples with <0.1% Sb at relatively high growth temperature of ~600 °C.

1. Structural properties

Ion channeling measurements showed that GaN films grown at 600 °C are single crystalline with a channeling yield χ_{min} ~ 0.04. With the incorporation of only 0.04% (~1.8×10^{19}/cm^3) of Sb, χ_{min} increases to 0.18, suggesting that small amount of Sb atoms strongly disrupt the crystallinity of the GaN lattice. Figure 2 shows the microstructures of the films grown at ~600 °C both (a) undoped and (b) Sb doped (~0.04%) under Ga-rich condition (Ga BEP ~ 2.3×10^{-7} T). For the undoped GaN film, we observe a regular columnar structure. The high resolution image shows that this undoped layer has good crystallinity with a higher density of defects close to the GaN/sapphire interface. In contrast, the film grown with only 0.04% of Sb shows a non-columnar structure with high dislocation density. These microstructures are consistent with the observed high ion channeling yield of ~0.18.

The incorporation of Sb in GaN at T_g ~ 600 °C with increasing Sb BEP under Ga-rich (BEP ~ 2.3×10^{-7} T) and N-rich (BEP ~ 1.5×10^{-7} T) growth conditions is shown in Fig. 3. Over an order of magnitude higher Sb incorporation is observed for the N-rich growth condition. However, as seen in Fig. 3, for both Ga-rich and N-rich cases increasing Sb flux has very small effect on the total Sb content in the films. This can be understood by a low solubility limit of Sb in GaN with the excess Sb segregating to the surface and desorbing during the growth at this relatively high temperature of 600 °C. Hence, at T_g ~ 600 °C, ~0.7% of Sb can be incorporated in GaN under N-rich condition but only ~0.04% of Sb under Ga-rich condition.

2. Optical properties

Room temperature CL measurements were carried out on Sb doped GaN samples with dilute amount of Sb (<1%) grown at 600 °C. A broad luminescence at 2.0–2.5 eV with peak intensity at ~2.2 eV is observed for films with small amount of Sb. Fig. 4 shows a comparison of two CL spectra of GaN with no Sb and with ~0.04% Sb grown at ~600 °C under similar Ga flux. Note that only the band edge luminescence of ~3.4 eV is observed for the sample without Sb. This suggests that the broad CL peak can be attributed to incorporation of the Sb. Wu *et al.*[11] have shown that the composition dependence of the bandgap in GaNAs alloys can be explained by the BAC model with the localized As level E_{As} ~ 0.62 eV above the VBM of

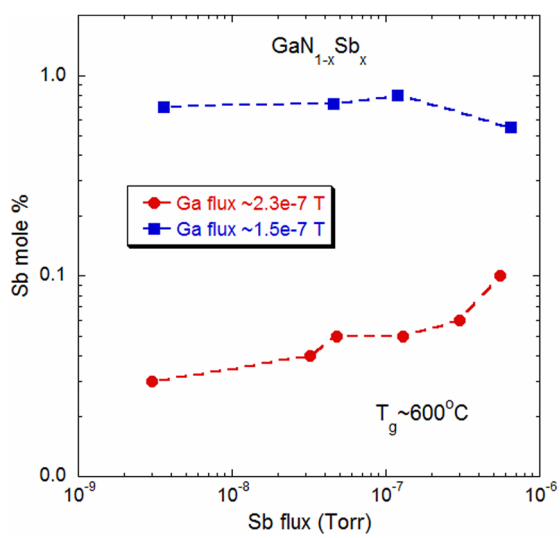

FIG. 3. Sb incorporation as a function of Sb BEP for films grown at ~600 °C under N-rich and Ga-rich conditions.

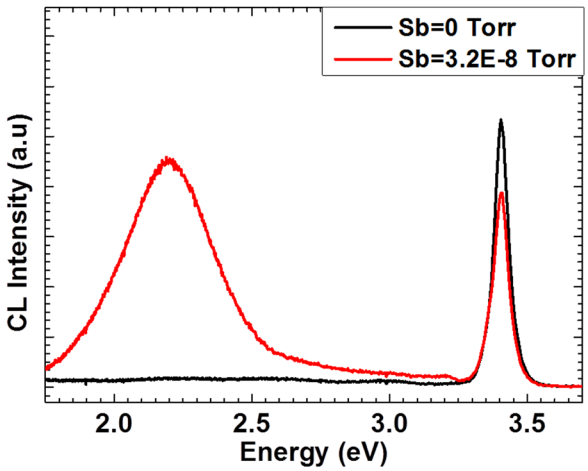

FIG. 4. Cathodoluminescence spectra of GaN thin films grown at ~600 °C with Sb BEP ~0 and 3.2×10^{-8} T, respectively. The sample grown with Sb flux has a Sb content of ~0.04%.

GaN. Photoluminescence measurements on As doped GaN by Foxon *et al*. showed a broad luminescence from 2.23 to 2.9 eV with peak intensity at ~2.65 eV.[9] Considering a likely ~0.1 eV Stokes shift in the PL peak, this places the $E_{As} \sim 0.65$ eV, in good agreement with the value obtained by Wu *et al*. Since the electronegativity difference between Sb and N is larger than between As and N, it is expected that Sb-derived localized levels lie higher above the valence band edge than that the As levels. Again, assuming the Stokes shift of 0.1 eV places the Sb level at $E_{Sb} \sim 1.1$ eV above the VBM of GaN. This is in a good agreement with the value extrapolated from the position of the Sb level at 0.9 eV below the VBM in GaAs.[13] However, it is important to note that the CL peak at 2.2 eV coincides with the commonly observed "yellow" luminescence in GaN that has been attributed to native defects or defect complexes. Since incorporation of Sb affects the crystalline quality of the films, it is therefore possible that Sb levels and native defects contribute to the observed CL. The nature of this CL peak will be discussed later in this paper together with our optical absorption results for $GaN_{1-x}As_x$ alloys grown at lower temperature with higher Sb contents.

C. Low temperature growth (80–500 °C)

1. Effect of growth temperature on the microstructure

At low growth temperatures, the Sb incorporation in $GaN_{1-x}Sb_x$ is greatly enhanced. As shown in Fig. 1, the Sb content increases with decreasing temperature and tends to saturate at ~300 °C for N-rich and ~500 °C for Ga-rich growth. In contrast, in the case of As in $GaN_{1-x}As_x$, lowering the growth temperature monotonically increases the As content in the film down to the lowest temperature of 100 °C.

It has been previously reported that due to the strong ionic nature of GaN, a c-axis oriented polycrystalline hexagonal GaN phase dominates even at the lowest growth temperature of 80 °C.[2,17,18] TEM investigations reveal that GaN films grown at 80 °C are columnar, with average column widths of 10 nm near the sapphire interface and 14 nm near the surface. The SAD pattern shows clear polycrystalline rings. The intensity of the XRD (0002) peak decreases as more Sb is incorporated into the lattice by increasing the Sb flux. At the growth temperature of 80 °C, the samples become less crystalline with increasing Sb content and eventually become entirely amorphous with ~6% of Sb. High resolution TEM investigations reveal that the columnar structure that was observed in samples with low Sb content is completely absent for films with higher Sb (>6%). Films with >6% of Sb exhibits a primarily amorphous structure with small ~2–5 nm inclusions of crystalline grains. From the thickness measured by cross-sectional TEM and the areal density from RBS, we calculated the density of the amorphous $GaN_{1-x}Sb_x$ film with ~6% Sb to be ~84% of the corresponding crystalline phase.

Figure 5 shows XRD patterns of $GaN_{1-x}Sb_x$ sample grown at different substrate temperatures with similar Ga and Sb BEP and with Sb content of ~4%–5%. At this Sb content, films grown below 100 °C are entirely amorphous. At $T_g \sim 135$ °C, the film becomes partially crystalline as evidenced by the weak and broad (0002) diffraction peak. This diffraction peak is most likely coming from small crystalline grains within the amorphous matrix. At higher growth temperatures, the (0002) peak intensity increases, indicating that a larger fraction of the film is crystalline with larger grain sizes. At the even higher growth temperature of 470 °C, the (0002) diffraction peak becomes strong, suggesting growth of a fully crystalline film that is preferentially oriented to the growth direction of the substrate. However, at higher Sb content of ~7%, the films remain amorphous even at the growth temperature as high as 285 °C. Phase separation occurs at the high growth temperature of 470 °C when the Sb content increases to $x > 0.06$ with a clearly visible (210) zinc blende GaSb peak at $2\theta \sim 32.6°$ as shown in the inset of Fig. 5.

Cross sectional TEM images and SAD patterns for samples grown at (a) 80 °C, (b) 195 °C, and (c) 470 °C with similar Ga and Sb fluxes and with Sb content in the range of 4%–6%

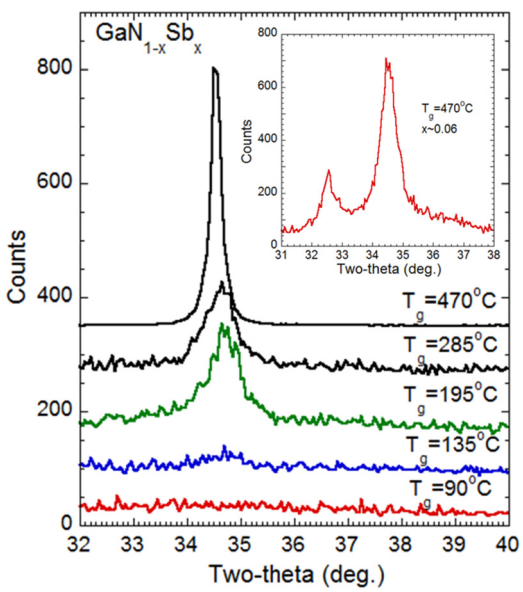

FIG. 5. XRD patterns of $GaN_{1-x}Sb_x$ sample grown at different substrate temperature with similar Ga and Sb BEP with Sb content ~4%–5.0%. The inset shows XRD pattern from a sample grown at 470 °C with a higher Sb content of 6%.

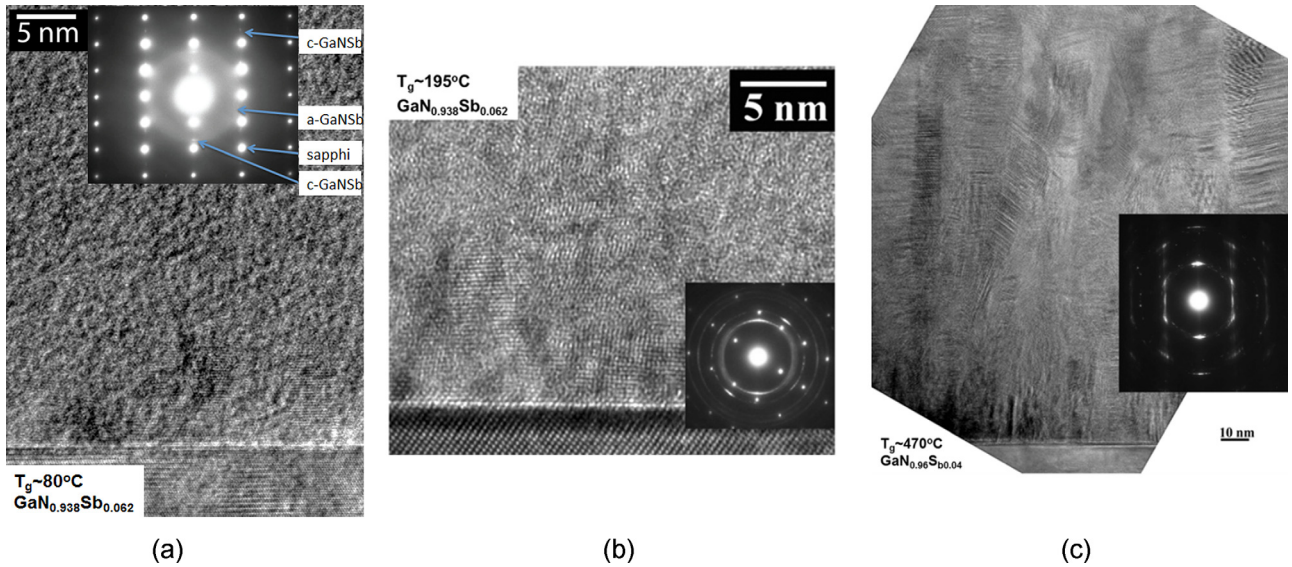

FIG. 6. Cross section TEM images and SAD patterns of samples grown at (a) 80 °C, (b) 195 °C, and (c) 470 °C grown with similar Ga and Sb flux with Sb content in the range of 4%–6%.

are shown in Fig. 6. At the low growth temperature of 80 °C, the sample with 6.2% Sb appears to be entirely amorphous. The columnar structure that was observed in the sample with lower Sb content is completely absent in this film. The diffuse rings in the SAD pattern shown in Fig. 6(a) confirm that the film is primarily amorphous, in good agreement with the XRD results. The microstructure of the film with 6.2% Sb grown at 195 °C shown in Fig. 6(b) reveals that the film has both crystalline grains of ~5 nm size and amorphous regions. SAD patterns also show crystalline diffraction rings indicating polycrystalline grains as well as an amorphous ring. These results are consistent with the XRD pattern of the sample showing only a weak (0002) GaNSb diffraction peak. At the high growth temperature of 470 °C, both the TEM image and the SAD pattern indicate a polycrystalline film.

2. Effect of Ga and Sb flux

Sb incorporation and the overall III:V ([Ga]/([N] + [Sb])) ratio depends quite strongly on the Ga flux during growth, particularly at low growth temperature. Fig. 7 shows the Ga flux dependence on the Sb concentration in mol. % and the III/V atomic ratio, [Ga]/([Sb] + [N]) of $GaN_{1-x}Sb_x$ films grown at substrate temperature of 80 °C at a fixed Sb BEP of 3.2×10^{-8} T. As is seen in Fig. 7, increasing Ga flux at a fixed Sb flux results in decreased Sb incorporation and a corresponding increase in the III/V ratio of the film. Under these growth conditions, stoichiometric III:V material with Sb mole fractions of $x \sim 0.05$ can be obtained with a Ga flux of $\sim 2 \times 10^{-7}$ Torr.

Figures 8(a) and 8(b) show the Sb incorporation and III:V ratio for $GaN_{1-x}Sb_x$ films grown at a substrate temperature of 80 °C with increasing Sb BEP under N-rich (Ga BEP ~ 1.6×10^{-7} Torr) and Ga-rich (Ga BEP ~ 2.2×10^{-7} Torr) conditions, respectively. Note that at the low growth temperature $T_g \sim 80$ °C, the incorporation of Sb increases linearly with Sb BEP independent of the Ga BEP. Under the Ga-rich growth condition, $GaN_{1-x}Sb_x$ films with III:V ratio of unity can be obtained with Sb BEP up to 8×10^{-8} Torr with up to 10 mol. % Sb. However, under N-rich growth condition, stoichiometric films can be obtained only for Sb BEP ~ 2×10^{-8} Torr, giving rise to ~4 mol. % of Sb in the film. This suggests that Ga-rich growth conditions are required to incorporate high concentrations of Sb into $GaN_{1-x}Sb_x$ while still maintaining a good film stoichiometry. However, for low Sb flux, a Ga-rich growth may also favor the incorporation of Ga antisites N_{Ga}. Such N_{Ga} antisites may introduce deep levels within the gap.

3. Optical properties of $GaN_{1-x}Sb_x$

The absorption coefficient α of $GaN_{1-x}Sb_x$ films was measured using transmission and reflection measurements. Figure 9(b) shows α for $GaN_{1-x}Sb_x$ films with increasing Sb

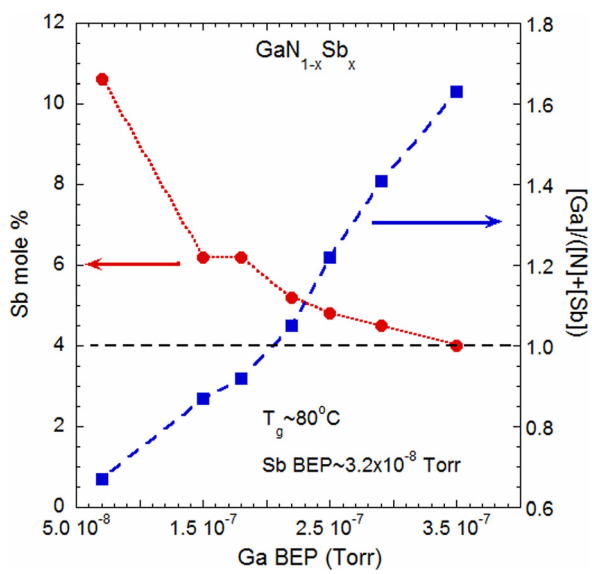

FIG. 7. Concentrations of Sb in mol. % together with the III/V atomic ratio, [Ga]/([Sb] + [N]) of the films grown at substrate temperature of 80 °C at a fixed Sb BEP of 3.2×10^{-8} T with increasing Ga flux.

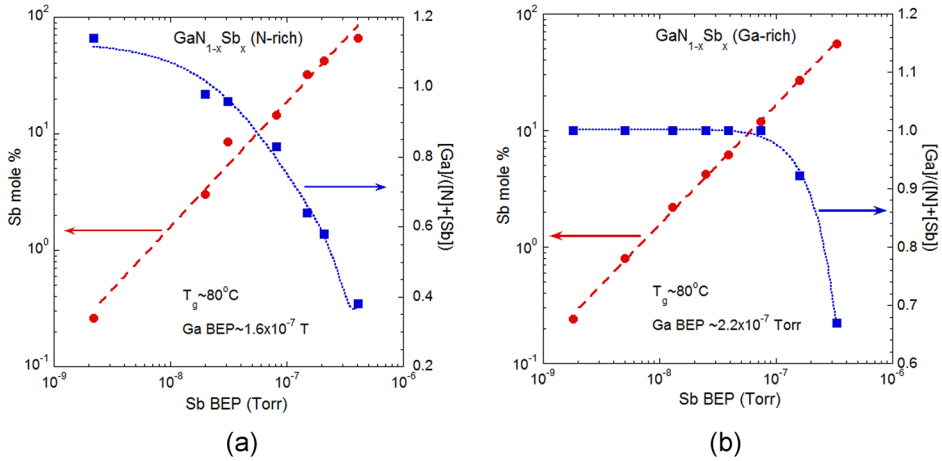

FIG. 8. Concentrations of Sb in mol. % together with the III/V atomic ratio, [Ga]/([Sb] + [N]) of the films grown at substrate temperature of 80 °C with increasing Sb flux for (a) N-rich (Ga BEP ~ 1.6×10^{-7} T), and (b) Ga-rich (Ga BEP ~ 2.2×10^{-7} T) conditions.

content grown at 80 °C under N-rich growth condition. The inset of Fig. 9(b) shows the band structure of a $GaN_{0.95}Sb_{0.05}$ alloy calculated using the BAC model with E_{Sb} at 1.1 eV above the VBM of GaN and a coupling parameter $C_{GaN\text{-}Sb}$ of 1.4 eV. A monotonic increase of the sub-bandgap optical absorption starting with photon energies of less than 2 eV is observed with increasing Sb content. As illustrated in the inset of Fig. 9(b), this absorption can be attributed to optical transitions from the Sb-derived band (E_+) to the conduction band. It is very weak at low Sb concentrations but starts to dominate when the Sb content reaches a few mol. %. Note that although the film becomes amorphous for $x > 0.07$, the optical absorption shows a well-developed, relatively sharp absorption edge. In contrast, a $GaN_{1-x}Sb_x$ ($x = 0.062$) film grown under Ga-rich conditions (Ga BEP $> 2.2 \times 10^{-7}$ T) exhibits a strong absorption at energy as low as 1 eV. It appears that the strong low energy absorption for Ga-rich grown films has a different origin. We believe that it may arise from non-stoichiometric defects forming a midgap defect band. Hall effect and thermopower measurements show that samples grown under the Ga-rich condition are p-type, indicating that these excess Ga-related defects are acceptors.

Because of the complex, composition-dependent valence band structure, the standard method to determine the band gap using a linear fit to α^2 as a function of photon energy cannot be applied at low Sb levels. Here, we adopted the fitting procedure used by Mayer *et al.* to evaluate the absorption coefficient in $ZnO_{1-x}Se_x$ HMA alloys.[21] We consider optical transitions from three valence bands: the Sb derived impurity band to conduction band (E_+), Sb spin orbit split band to conduction band (E_+^{SO}), and the GaN matrix-like band to conduction band (E_-). Also, to account for broadening in the bands inherent to the BAC model and arising from localized composition fluctuations, we convolve the energy dependent joint optical density of states with a Gaussian function at each k value. The expression for the total absorption coefficient α can be expressed as the sum of optical absorptions to the conduction band from three valence bands (g_+, $g_{+,SO}$, and g_-),

$$\alpha(\hbar\omega) = \alpha_0\left(\frac{2}{3}g_+(\hbar\omega) + \frac{1}{3}g_{+,SO}(\hbar\omega) + g_-(\hbar\omega)\right), \quad (2)$$

where the transitions are weighted with the degeneracy factors and α_0 is a scaling constant.

Good agreement with the experiment is obtained by a single set of the VBAC parameters: the coupling constant, $C_{GaN\text{-}Sb} = 1.4$ eV and the localized Sb level, $E_{Sb} = 1.1$ eV above the valence band. As discussed above, this value is in good agreement with E_{Sb} estimated from the CL peak observed in high temperature grown Sb doped GaN materials shown in Fig. 4 and from the extrapolation of the E_{Sb} value from GaAsSb.[13] An example of the fitting is shown in Fig. 9(a) for a sample with $x = 0.144$. Bandgap energies obtained by fitting experimental absorption coefficient using these

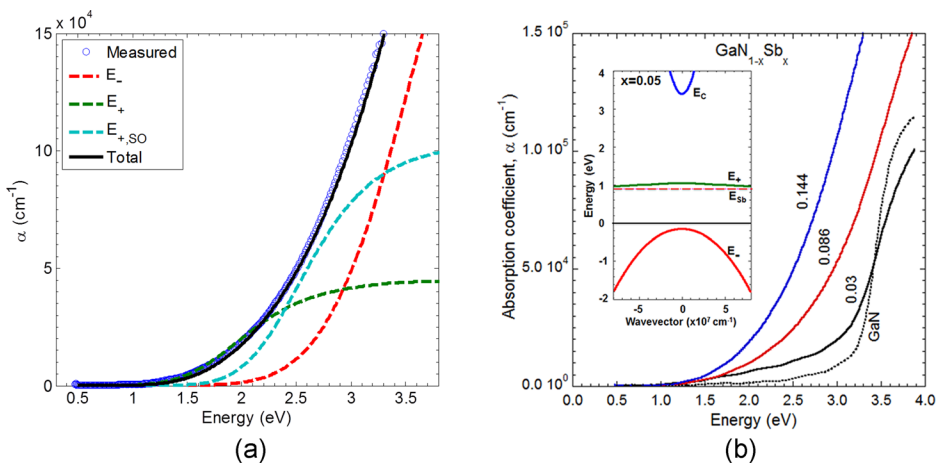

FIG. 9. (a) Absorption coefficient, α for the $GaN_{1-x}Sb_x$ film $x = 0.144$ (circles) and the theoretical fit calculated according to Eq. (1) showing contributions of the absorption coefficient from the three valence bands. (b) α for $GaN_{1-x}Sb_x$ films with increasing Sb content grown at 80 °C under N-rich growth condition. The inset shows the band structure of a $GaN_{0.95}Sb_{0.05}$ alloy calculated using the BAC model with E_{Sb} at 1.1 eV above the VBM of GaN and a coupling parameter $C_{GaN\text{-}Sb}$ of 1.4 eV.

parameters for $GaN_{1-x}Sb_x$ films grown under N-rich conditions at a temperature range of 80–470 °C are shown in Fig. 10. Bandgap energies for GaSb-rich alloys with up to 1% of N were taken from Jefferson *et al.*[22] and Veal *et al.*[23] A large drop of the absorption edge energy (from 3.4 to ~2.5 eV) is already observed for films with only a small amount of Sb (~3%). Since the conduction band edge of GaSb is only ~0.3 eV lower than that of GaN, the change in the band gap of the $GaN_{1-x}Sb_x$ alloys comes primarily from the modification of valence band.

The dependence of the fundamental band of $GaN_{1-x}Sb_x$ in the whole composition range was calculated using the BAC model with the interpolation procedure proposed by Wu *et al.*[11] and the results are shown as the dashed line in Fig. 10. In this calculation, the values of $E_{Sb} = 1.1$ eV and $C_{GaN\text{-}Sb} = 1.4$ eV obtained from fitting the absorption coefficient are used for valence band anticrossing on the GaN-rich side, while $E_N = 0.4$ eV above the GaSb CBM and $C_{GaSb\text{-}N} = 2.7$ eV are used for the conduction band anticrossing on the GaSb-rich side.[22] In the case of $GaN_{1-x}As_x$ HMAs, the As energy level in GaN E_{As} and the coupling parameter $C_{GaN\text{-}As}$ have been estimated to be ~0.62 eV above the VBM of GaN and 0.75 eV, respectively.[11] Given the larger mismatch between Sb and N, the larger values of E_{Sb} and $C_{GaN\text{-}Sb}$ are reasonable. The advantage of the BAC model is that it separately calculates the energy of the CBM and the VBM on the absolute scale. The corresponding CBM and VBM (E_+) calculated using the BAC model as a function GaSb mole fraction are shown in the inset of Fig. 10. It should be noted that the strong decrease in the bandgap of dilute Sb alloys is attributed to the large upward shift of the VBM. Also, as is seen in Fig. 10 the CBM and VBM of $GaN_{1-x}Sb_x$ with $x \sim 0.15$ still straddle the redox potentials for pH = 2 (indicated as dashed lines). At this composition $E_g \sim 1.8$ eV, making this alloy a favorable candidate as a photoelectrode for spontaneous PEC water splitting.

Fig. 10 shows that the calculated bandgap dependence on composition is in very good agreement with the experimental values, especially for Sb contents <30%. For samples with Sb content >30%, the calculated values are consistently smaller than the experimental values. This can be attributed to the fact that RBS measures the total Sb concentration that may be higher than the actual amount of Sb substituting the N site and contributing to the modification of the band structure of the alloy. This difference is expected to be more severe for high Sb contents. We note that the BAC model is a phenomenological model developed for the substitution of dilute amount of mismatched anions. The calculated bandgap shown in Fig. 10 is a composition weighted interpolation of the BAC model and thus is expected to be less accurate for the alloys in the middle range of compositions. Furthermore, since the model is developed for crystalline materials, deviation of the experimental results from the BAC calculations found for the amorphous alloys with high Sb content is not unexpected.

Figure 11 shows a schematic of the band offsets of GaN, GaAs, and GaSb with the positions of E_{As} in GaN, E_{Sb} in GaAs, and GaN and E_N in GaSb and GaAs. We adopt the electron affinities and bandgaps of the various materials from the collections in the website http://www.ioffe.ru/SVA/NSM/Semicond/. We plot the energies of these localized levels with an energy uncertainty of ±0.1 eV since they were measured by different experimental methods and in materials

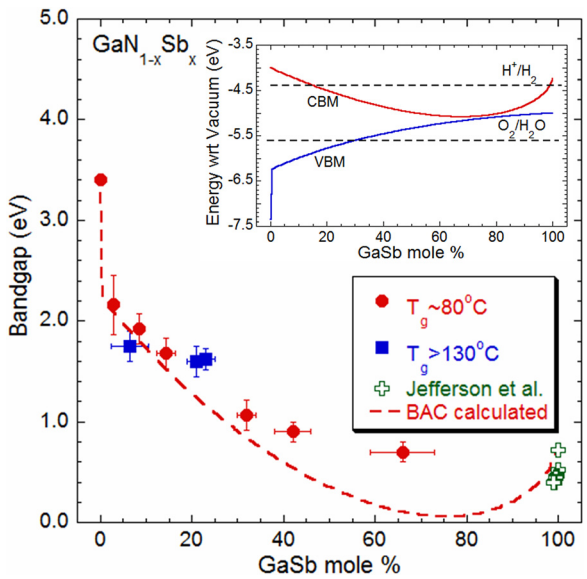

FIG. 10. Bandgap energy obtained by fitting the absorption coefficient with the valence band anticrossing for $GaN_{1-x}Sb_x$ films grown under N-rich conditions at a temperature range of 80–470 °C. Bandgap energies for GaSb-rich alloys with up to 1% of N were taken from Jefferson *et al.*[22] The dashed line shows the interpolated bandgap calculated according to the BAC model. The BAC calculated CBM and VBM (E_+) as a function GaSb mole fraction are shown in the inset with the Redox levels for pH = 2 indicated as dashed lines.

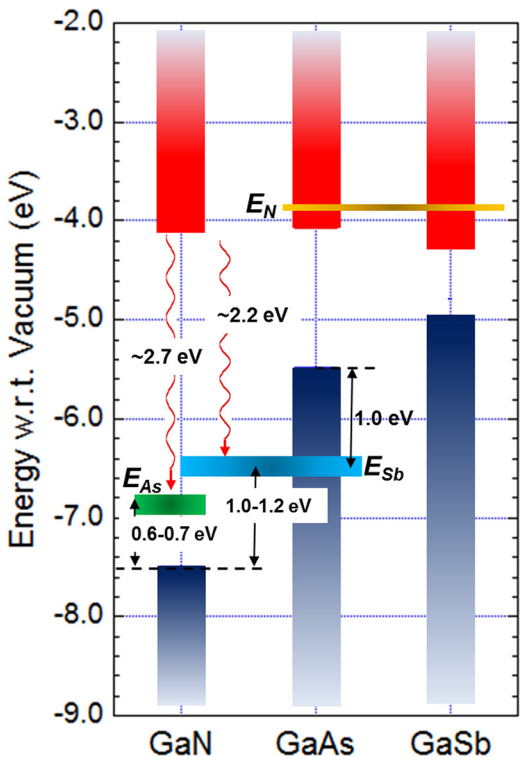

FIG. 11. A schematic diagram of the band offsets of GaN, GaAs, and GaSb with the locations of E_{As} in GaN, E_{Sb} in GaAs and GaN, and E_N in GaSb obtained from various references as mentioned in this manuscript.

grown under different conditions. The location of E_{As} in GaN is taken from the PL results[9] and the BAC fitting of the absorption edge,[11] while E_{Sb} in GaN is adopted from the BAC fitting of the bandgap in dilute $GaSb_xAs_{1-x}$ alloys.[13] The 2.2 eV luminescence we observed in our samples is very close to the energy separation between the conduction band to the E_{Sb} ($\sim$2.3 eV assuming $E_{Sb} = 1.1$ eV). Hence, this $\sim$2.2 eV luminescence peak may indeed be associated with optical transitions between CBM of GaN and E_{Sb}.

IV. CONCLUSION

We have carried out a systematic study on $GaN_{1-x}Sb_x$ highly mismatched alloys grown by low temperature MBE. The effects of growth temperature, Ga flux, and Sb flux on the incorporation of Sb, film structure, and optical properties of the alloys are investigated. We found that at the growth temperature of 80 °C and $x > 6\%$, $GaN_{1-x}Sb_x$ becomes primarily amorphous with small crystallites of 2–5 nm. The Sb content in the $GaN_{1-x}Sb_x$ film for a given Sb flux is rather insensitive to the growth temperature at a growth temperature below 400 °C. Despite the range of microstructures found for $GaN_{1-x}Sb_x$ alloys with different composition, a well-developed absorption edge shifts from 3.4 eV (GaN) to close to 2 eV for samples with a small amount of Sb (<5 at. %). Luminescence from dilute $GaN_{1-x}Sb_x$ alloys grown at high temperature, and the bandgap energies for alloys with higher Sb contents are consistent with a E_{Sb} level at $\sim$1.1 eV above the valence band of GaN. Our work demonstrates that a large range of direct bandgap energies from 3.4 eV to below 1.0 eV can be achieved for $GaN_{1-x}Sb_x$ HMAs grown at low temperature.

ACKNOWLEDGMENTS

The MBE growth at the University of Nottingham was undertaken with support from the EPSRC (EP/I004203/1) and by the US Army under cooperative Agreement No. W911NF-12-2-0003. RBS and optical measurements performed at LBNL were supported by the U.S. Department of Energy, Office of Science, Basic Energy Sciences, Materials Sciences and Engineering Division. The characterization work at Strathclyde University was funded by EPSRC Grant No. EP/I004203/1.

[1]S. V. Novikov, C. R. Staddon, C. T. Foxon, K. M. Yu, R. Broesler, M. Hawkridge, Z. Liliental-Weber, W. Walukiewicz, J. Denlinger, and I. Demchenko, J. Vac. Sci. Technol. B **28**, C3B12 (2010).
[2]K. M. Yu, S. V. Novikov, R. Broesler, I. N. Demchenko, J. D. Denlinger, Z. Liliental-Weber, F. Luckert, R. W. Martin, W. Walukiewicz, and C. T. Foxon, J. Appl. Phys. **106**, 103709 (2009).
[3]W. Walukiewicz, W. Shan, K. M. Yu, J. W. Ager III, E. E. Haller, I. Miotkowski, M. J. Seong, H. Alawadhi, and A. K. Ramdas, Phys. Rev. Lett. **85**, 1552 (2000).
[4]W. Shan, W. Walukiewicz, J. W. Ager III, E. E. Haller, J. F. Geisz, D. J. Friedman, J. M. Olson, and S. R. Kurtz, Phys. Rev. Lett. **82**, 1221 (1999).
[5]W. Walukiewicz, W. Shan, J. Wu, K. M. Yu, and J. W. Ager III, in *Dilute Nitride Semiconductors*, edited by M. Henini (Elsevier, Oxford, UK, 2005), Chap. 10.
[6]K. Uesugi, N. Marooka, and I. Suemune, Appl. Phys. Lett. **74**, 1254 (1999).
[7]*Physics of Dilute III–V Nitride Semiconductors and Material Systems: Physics and Technology*, edited by A. Erol (Springer-Verlag, Berlin, 2008).
[8]W. Walukiewicz, K. Alberi, J. Wu, W. Shan, K. M. Yu, and J. W. Ager III, in *Physics of Dilute III–V Nitride Semiconductors and Material Systems: Physics and Technology*, edited by A. Erol (Springer-Verlag, Berlin, 2008), Chap. 3.
[9]C. T. Foxon, I. Harrison, S. V. Novikov, A. J. Winser, R. P. Campion, and T. Li, J. Phys.: Condens. Matter **14**, 3383 (2002).
[10]A. Kimura, C. A. Paulson, H. F. Tang, and T. F. Kuech, Appl. Phys. Lett. **84**, 1489 (2004).
[11]J. Wu, W. Walukiewicz, K. M. Yu, J. D. Denlinger, W. Shan, J. W. Ager, A. Kimura, H. F. Tang, and T. F. Kuech, Phys. Rev. B **70**, 115214 (2004).
[12]K. M. Yu, W. Walukiewicz, J. Wu, W. Shan, J. W. Beeman, M. A. Scarpulla, O. D. Dubon, and P. Becla, Phys. Rev. Lett. **91**, 246403 (2003).
[13]K. Alberi, J. Wu, W. Walukiewicz, K. M. Yu, O. D. Dubon, S. P. Watkins, C. X. Wang, X. Liu, Y. J. Cho, and J. Furdyna, Phys. Rev. B **75**, 045203 (2007).
[14]S. V. Novikov, C. R. Staddon, A. V. Akimov, R. P. Campion, N. Zainal, A. J. Kent, C. T. Foxon, C.-H. Chen, K. M. Yu, and W. Walukiewicz, J. Cryst. Growth **311**, 3417–3422 (2009).
[15]K. M. Yu, S. V. Novikov, R. Broesler, Z. Liliental-Weber, A. X. Levander, V. M. Kao, O. D. Dubon, J. Wu, W. Walukiewicz, and C. T. Foxon, Appl. Phys. Lett. **97**, 101906 (2010).
[16]R. Sheetz, E. Richter, A. N. Andriotis, S. Lisenkov, C. Pendyala, M. K. Sunkara, and M. Menon, Phys. Rev. B **84**(7), 075304 (2011).
[17]K. M. Yu, W. L. Sarney, S. V. Novikov, D. Detert, R. Zhao, J. Denlinger, S. P. Svensson, O. D. Dubon, W. Walukiewicz, and C. T. Foxon, Appl. Phys. Lett. **102**, 102104 (2013).
[18]W. L. Sarney, S. P. Svensson, S. V. Novikov, K. M. Yu, W. Walukiewicz, and C. T. Foxon, "$GaN_{1-x}Sb_x$ highly mismatched alloys grown by low temperature molecular beam epitaxy under Ga-rich conditions," J. Cryst. Growth **383**, 95 (2013).
[19]A. X. Levander, K. M. Yu, S. V. Novikov, J. D. Denlinger, A. Tseng, C. T. Foxon, O. D. Dubon, J. Wu, and W. Walukiewicz, Appl. Phys. Lett. **97**, 141919 (2010).
[20]S. V. Novikov, T. Li, A. J. Winser, R. P. Campion, C. R. Staddon, C. S. Davis, I. Harrison, and C. T. Foxon, Phys. Status Solidi B **228**, 223 (2001).
[21]M. A. Mayer, D. T. M. Speaks, K. M. Yu, S. S. Mao, E. E. Haller, and W. Walukiewicz, Appl. Phys. Lett. **97**, 022104 (2010).
[22]P. H. Jefferson, T. D. Veal, L. F. J. Piper, B. R. Bennett, C. F. McConville, B. N. Murdin, L. Buckle, G. W. Smith, and T. Ashley, Appl. Phys. Lett. **89**, 111921 (2006).
[23]T. D. Veal, L. F. J. Piper, S. Jollands, B. R. Bennett, P. H. Jefferson, P. A. Thomas, C. F. McConville, B. N. Murdin, L. Buckle, G. W. Smith, and T. Ashley, Appl. Phys. Lett. **87**, 132101 (2005).